Pharmacological Reports 71 (2019) 1006–1013

Contents lists available at ScienceDirect

Pharmacological Reports

journal homepage: www.elsevier.com/locate/pharep

Original article

# Penta-acetyl geniposide induces apoptosis of fibroblast-like synoviocytes from adjuvant-induced arthritis rats *in vitro*, associated with inhibition of NF-κB activation

Li Cai[a,1], Chun-mei Li[b,1], Wei-na Chen[b], Yuan-ye Qiu[c], Yan-li Guo[d], Rong Li[b,c,*]

[a] Department of Pathology, School of Basic Medicine, Anhui Medical University, Hefei, Anhui Province, China
[b] School of Pharmacy, Anhui Medical University, Hefei, Anhui Province, China
[c] School of Pharmacy, Macau University of Science and Technology, Macau, China
[d] Anhui Provincial Institute of Food and Drug Inspection, Hefei, Anhui Province, China

ARTICLE INFO

*Article history:*
Received 9 November 2018
Received in revised form 9 May 2019
Accepted 21 May 2019
Available online 22 May 2019

*Keywords:*
Penta-acetyl geniposide
Apoptosis
Adjuvant-induced arthritis
Fibroblast-like synoviocytes
NF-κB signaling pathway

ABSTRACT

*Background:* Approaches promoting fibroblast-like synoviocytes (FLS) apoptosis are considered as a meaningful strategy for rheumatoid arthritis (RA) treatment. We have previously reported the anti-arthritic effect of penta-acetyl geniposide ($(Ac)_5GP$, an active derivative of geniposide) on adjuvant-induced arthritis (AIA) rats *in vivo*. The present study aimed to investigate the pro-apoptotic effect of $(Ac)_5GP$ on AIA FLS *in vitro* and the underlying molecular mechanisms.
*Methods:* Rat AIA was induced by complete Freund's adjuvant, and FLS were primary-cultured from synovial tissues. AIA FLS were treated with $(Ac)_5GP$ (50, 100 and 200 μM) for 48 h and cell proliferation and apoptosis were respectively examined. The involvement of apoptosis-related proteins (Bax, Bcl-2 and caspase 3) and nuclear factor kappa B (NF-κB) signaling pathway was checked.
*Results:* $(Ac)_5GP$ inhibited the viability of AIA FLS and reduced the percentage of Ki67-positive cells in AIA FLS. Particularly, $(Ac)_5GP$ promoted AIA FLS apoptosis *in vitro* by inducing apoptotic nuclear morphology, facilitating DNA ladder formation and increasing percentages of both early and late apoptotic cells. $(Ac)_5GP$ treatment on AIA FLS decreased Bcl-2 protein level whereas increased the levels of Bax and caspase 3 proteins. Moreover, $(Ac)_5GP$ reduced the degradation and phosphorylation of IκBα, down-regulated NF-κB p65 protein level in nucleus and inhibited NF-κB p65 nuclear translocation.
*Conclusions:* $(Ac)_5GP$ had a potent pro-apoptotic effect on AIA FLS *in vitro*, which is associated with regulating apoptosis-related proteins and inhibiting NF-κB activation.


## Introduction

Rheumatoid arthritis (RA) is a kind of chronic autoimmune disease featured by synovitis, synovial hyperplasia and inevitable joint destruction [1]. Fibroblast-like synoviocytes (FLS) as the main cells involved in RA pathogenesis exhibit multiple tumor-like features, such as excessive proliferation, inadequate apoptosis and high invasiveness [2]. It is generally accepted that the unbalance between proliferation and apoptosis of RA FLS results in synovial hyperplasia, finally contributes to pannus formation, synovial inflammation and extracellular matrix degradation [3]. Thus, promoting FLS apoptosis and consequently suppressing synovial hyperplasia might be considered as a potential therapeutic approach for RA disease [4].

Traditional Chinese medicine and herbal medicine are desirable in RA treatment, due to the advantages of safety and tolerability over current clinical drugs for RA [5]. Geniposide (an iridoid glycoside compound) isolated from *Gardenia jasminoides Ellis* exerts many pharmacological activities including anti-inflammatory, neuro-protective, and anti-oxidant effect [6]. The anti-arthritic potential of geniposide on rats with adjuvant-induced arthritis (AIA) has already been reported [7]. However, the poor oral absorption and low bioavailability of geniposide restrict its further application in pharmaceutical field [8]. Among a series of geniposide derivatives, penta-acetyl geniposide ($(Ac)_5GP$, Fig. 1A), an acetylated derivative of geniposide, showed more effective anti-inflammatory activities than its parent compound geniposide [9]. Oral administration of $(Ac)_5GP$ inhibited the inflammation progress and the synovial hyperplasia in AIA rats, indicating an anti-arthritic effect of $(Ac)_5GP$

* Corresponding author.
*E-mail address:* aydlirong@163.com (R. Li).
[1] Li Cai and Chun-mei Li contributed equally to this work.

http://dx.doi.org/10.1016/j.pharep.2019.05.014
1734-1140/

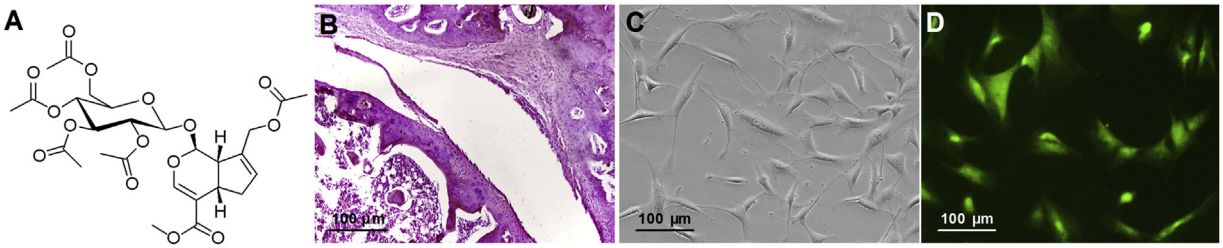


**Fig. 1.** (A) Chemical structure of $(Ac)_5GP$ ($C_{27}H_{34}O_{15}$, 598.55), (B) Histological examination of ankle joint sections from AIA rats by HE staining (×100), (C) Morphology of cultured cells (×100). (D) Positive VCAM-1 expression of cultured cells by immunofluorescence staining (×100).

*in vivo* [10]. It is interesting that $(Ac)_5GP$ was found to suppress the proliferation and induce the apoptosis of tumor cells, without influence on normal cells [11–13]. However, whether $(Ac)_5GP$ can affect the proliferation and apoptosis of RA FLS *in vitro* is still unknown and deserves further investigation.

This study purposed to explore the pro-apoptotic potential of $(Ac)_5GP$ on cultured AIA FLS. The expression of apoptosis-related proteins (Bax, Bcl-2 and caspase 3) and the activity of nuclear factor kappa B (NF-κB) signaling pathway were measured to demonstrate underlying molecular mechanisms. These experimental results may be helpful for illuminating the possible utility of $(Ac)_5GP$ in RA treatment.

## Materials and methods

### *Reagents*

Hoechst 33258, MTT and DAPI were purchased from Sigma Chemical Company (St. Louis, MO, USA). DMEM, trypsin and fetal bovine serum (FBS) were bought from Gibco Company (Carlsbad, CA, USA). Annexin V-FITC test kit, DNA extraction kit, and Cytoplasmic and nuclear extraction kit were purchased from Beyotime Biotechnology (Haimen, Jiangsu, China). Antibodies of vascular cell adhesion molecule-1 (VCAM-1, ab134047), NF-κB p65 (ab16502), IκBα (ab32518), caspase 3 (ab13847), Bax (ab32503), Bcl-2 (ab196495) and Ki67 (ab16667) were bought from Abcam (Cambridge, UK). The phospho-IκBα (p-IκBα, #2859) antibody was purchased from Cell Signaling Technology (Beverly, MA, USA). Complete Freund's adjuvant (CFA) was bought from Chondrex limited Company. $(Ac)_5GP$ (99% purity) was kindly provided by Dr. Wen-jian Tang (Anhui Medical University).

### *Rat AIA induction*

Sprague-Dawley rats (male, 120–130 g) were bought from the Laboratory Animals Center of Anhui Medical University and housed under standard laboratory conditions with free access to water and food. After 7-day acclimatization, rats were separated randomly into normal control group (10 rats) and AIA group (30 rats). 0.1 ml of CFA (containing 10 mg heat-killed mycobacteria per 1 ml paraffin oil) was intradermally injected to left hind paw to induce rat AIA [14], and an equal volume of physiological saline was given to normal rat. Rats were sacrificed on day 28 after CFA injection and histological examine of ankle joint was performed by hematoxylin and eosin (HE) staining. Synovial tissues from knee joints were isolated for preparing FLS. All procedures were permitted by the Ethic Committee and Animal Experimental Committee of Anhui Medical University, as accords with National Institutes of Health guide for the care and use of Laboratory animals (No. 8023, revised 1978).

### *Rat FLS culture and drug treatment*

Fresh synovial tissues were minced, rinsed, incubated in flat-bottomed bottles and cultured in DMEM media adding 10% FBS at 37 °C, 5% $CO_2$ for 7 days. The synovial pieces were discarded and adherent cells were further cultured for 3 days. The cell morphology and VCAM-1 staining were applied to identify the cultured cells. Most of the cultured cells after 2 passages contained a homogeneous population of FLS. FLS of passage 2–4 were used in the subsequent experiments. The cells were divided into normal FLS group (normal FLS without drug treatment), AIA FLS group (AIA FLS without drug treatment), normal FLS+$(Ac)_5GP$-treated groups (normal FLS with $(Ac)_5GP$ treatment at various concentrations), AIA FLS+$(Ac)_5GP$-treated groups (AIA FLS with $(Ac)_5GP$ treatment at various concentrations). In all experiments, the adherent FLS were treated with or without $(Ac)_5GP$ for 48 h before the specific test.

### *MTT assay*

FLS were seeded in 96-well plates ($5 \times 10^3$ cells/well) and incubated in DMEM at 37 °C, 5% $CO_2$. After adherence, normal FLS and AIA FLS were treated with $(Ac)_5GP$ (0, 12.5, 25, 50, 100, 200 and 400 μM) for 48 h. 20 μl of MTT solution (5 mg/ml) was added into each well and incubated for another 4 h. The supernatants were removed after centrifugation. When the formazan crystals were dissolved in dimethyl sulfoxide, the absorbance at 570 nm was measured by a microplate reader. The cell viability value was calculated as a ratio *versus* normal FLS group. The concentrations of $(Ac)_5GP$ (50, 100 and 200 μM) were adopted for treating AIA FLS in the following experiments based on MTT assay results.

### *Immunofluorescence assay*

FLS were adhered on coverslips placed in 6-well plates ($1 \times 10^5$ cells/well). Then, AIA FLS received 48 h of $(Ac)_5GP$ treatment according to experimental grouping. Cells were fixed by 4% paraformaldehyde and treated by 0.1%Triton X-100. Subsequently, cells were incubated with the primary antibody (Ki67 or NF-κB p65) at 4 °C overnight and the fluorescein-conjugated secondary antibody in dark for 1 h. Finally, cells were incubated with DAPI (1 μg/ml) in dark for 5 min. The coverslips were mounted by glycerin. The fluorescence was examined by Olympus IX71 equipped with fluorescent microscope and typical photos were taken. The number of Ki67-positive cells and total cells were manually counted in five different fields of each section, and the percentage of Ki67-positive cells was calculated. The mean of three sections per group was used as an independent data for statistical analysis.

### *Hoechst staining assay*

FLS were adhered on sterile coverslips placed in 6-well plates ($1 \times 10^5$ cells/well). The culture medium was removed and AIA FLS received 48 h of $(Ac)_5GP$ treatment. Cells were washed, fixed by 4% paraformaldehyde and further incubated by hoechst 33258

solution (10 μg/ml) in dark for 0.5 h. Cells were observed under a fluorescence microscope and representative photos were taken. The number of apoptotic cells with nuclear alterations and total cells were counted in five different fields of each section, and its percentage (%) was calculated. The mean of three sections per group was used as an independent data for statistical analysis.

*DNA extraction and agarose gel electrophoresis assay*

AIA FLS were treated with $(Ac)_5GP$ for 48 h. DNA was extracted by a DNA extraction kit according to the manufacturer instructions. An equal weight of DNA was loaded into 2% agarose gel adding ethidium bromide, and electrophoresed for 2 h at constant current (100 mA). DNA ladder formation was observed under ultraviolet illumination (260 nm). Cisplatin (10 μM) was used as a positive control in this assay.

*Flow cytometric assay*

FLS were cultured in 6-well plates ($1 \times 10^5$ cells/well) for 24 h adherence. Then, AIA FLS were treated with $(Ac)_5GP$ for 48 h. Cells were digested by trypsin, washed, centrifuged and suspended in binding buffer. 10 μl of PI solution and 5 μl of Annexin V-FITC solution were added into 400 μl of cell suspension. The mixed solution was incubated for 0.5 h at 4 °C in dark. Cells were examined using flow cytometry and the percentages of various cell subpopulations were analyzed by FlowJo 7.6 software.

*Western blot assay*

Cells were treated with RIPA lysis buffer containing protease inhibitor cocktails and proteins were isolated by an extraction kit. The protein levels in supernatant were measured by Bradford assay. The proteins were boiled, separated by SDS-PAGE and transferred to PVDF membrane by semidry electroblotting. PVDF membranes were blocked by 5% skim milk, incubated at 4 °C with the primary antibodies overnight, and incubated at 37 °C with HRP-conjugated secondary antibodies for 2 h. The same membrane was probed for β-actin or lamin B as the loading control. The blots were developed by Super Signal West Femto Trial Kit (Thermo Scientific, PA, USA). The protein bands were scanned and densitometrically quantified by Image J. The relative levels of target proteins were normalized by the internal control (β-actin or lamin B).

*Statistical analysis*

Statistical analysis was performed by SPSS 17.0 software. All experimental data were shown as mean ± standard error of the mean (SEM) obtained from three to five independent experiments performed in triplicate. Statistical analysis between groups was carried out by ANOVA, followed by Tukey HSD *post hoc* test, and $p < 0.05$ was considered to be statistically significant.

## Results

*Rat AIA evaluation and FLS identification*

The non-injected hind paw swelling in AIA rats was observed about on day 12 and reached to peak approximately on day 24 after CFA injection. In Fig. 1B, ankle joint sections from AIA rats exhibited many pathologic features resembling RA such as synovial hyperplasia, cartilage damage and inflammatory cells infiltration, suggesting that rat AIA model in this study was successfully established. The cultured cells after two passages showed a long spindle shape, which is accordant to the morphologic feature of FLS (Fig. 1C). The positive VCAM-1 expression by immunofluorescence staining further confirmed that the cultured cells were consistent with the intimal subpopulation of FLS (Fig. 1D).

*$(Ac)_5GP$ inhibited the proliferation of AIA FLS*

In Fig. 2A, MTT results revealed that there was no significant difference in the viability of normal FLS treated with $(Ac)_5GP$ at concentrations of 0, 12.5, 25, 50, 100, 200 and 400 μM for 48 h. The viability of AIA FLS was obviously higher than that of normal FLS. $(Ac)_5GP$ (12.5 and 25 μM) showed no obvious effect on AIA FLS viability, whereas $(Ac)_5GP$ (50, 100, 200 and 400 μM) remarkably reduced AIA FLS viability as compared with AIA FLS group. The concentrations of $(Ac)_5GP$ (50, 100 and 200 μM) were applied for the following experiments in AIA FLS since there was no statistical difference between 200 μM and 400 μM concentration. We also assayed the percentage of Ki67-positive cells in various groups by immunofluorescence assay (Fig. 2B, C). The percentage of Ki67-positive cells in AIA FLS group was much higher than that in normal FLS group. $(Ac)_5GP$ (50, 100 and 200 μM) significantly reversed the increased percentage of Ki67-positive cells in a dose-dependent manner. The above-mentioned results suggested that $(Ac)_5GP$ inhibited the proliferation of AIA FLS *in vitro*, without affecting the normal FLS.

*$(Ac)_5GP$ induced apoptotic nuclear morphology in AIA FLS*

Hoechst staining was applied to detect the apoptotic nuclear morphology (Fig. 3). The nuclei of most normal FLS were uniformly stained and round. This similar phenomenon was observed in AIA FLS and only a few cells showed mild nuclear alteration, indicating insufficient apoptosis of AIA FLS. In contrast, the apoptotic nuclear morphology including nuclear fragmentation and chromatin condensation was observed in $(Ac)_5GP$ (50, 100 and 200 μM)-treated groups at different degrees. The statistical analysis confirmed that $(Ac)_5GP$ dose-dependently increased the percentage of apoptotic cells with nuclear alterations compared with AIA FLS group.

*$(Ac)_5GP$ facilitated the formation of DNA ladder pattern in AIA FLS*

DNA agarose gel electrophoresis was used to check the formation of DNA ladder pattern (Fig. 4). DNA fragmentation was almost negligible in AIA FLS group, while DNA ladder pattern was embodied in cisplatin (positive control)-treated group. Similar DNA ladder pattern could be found in AIA FLS treated with $(Ac)_5GP$ (50,100 and 200 μM), suggesting that $(Ac)_5GP$ is able to induce AIA FLS apoptosis.

*$(Ac)_5GP$ increased AIA FLS apoptosis detected by flow cytometric assay*

The pro-apoptotic effect of $(Ac)_5GP$ was further confirmed by flow cytometer with Annexin V-FITC/PI staining (Fig. 5). Analysis of cell populations displayed various cell subpopulations, including healthy cells (Annexin V-FITC$^-$/PI$^-$), early apoptotic cells (Annexin V-FITC$^+$/PI$^-$), late apoptotic cells (Annexin V-FITC$^+$/PI$^+$) and necrotic cells (Annexin V-FITC$^-$/PI$^+$). The percentages of healthy cells in $(Ac)_5GP$ (50, 100 and 200 μM)-treated groups were all significantly decreased as compared with AIA FLS group. The percentages of early apoptotic cells and late apoptotic cells in AIA FLS were only a little higher than those in normal FLS, with no statistical significance, indicating that AIA FLS displayed an inadequate cell apoptosis. $(Ac)_5GP$ dose-dependently increased the percentages of both early and late apoptotic cells in AIA FLS. The percentages of necrotic cells in all groups were very low and there were no significant differences among all groups.

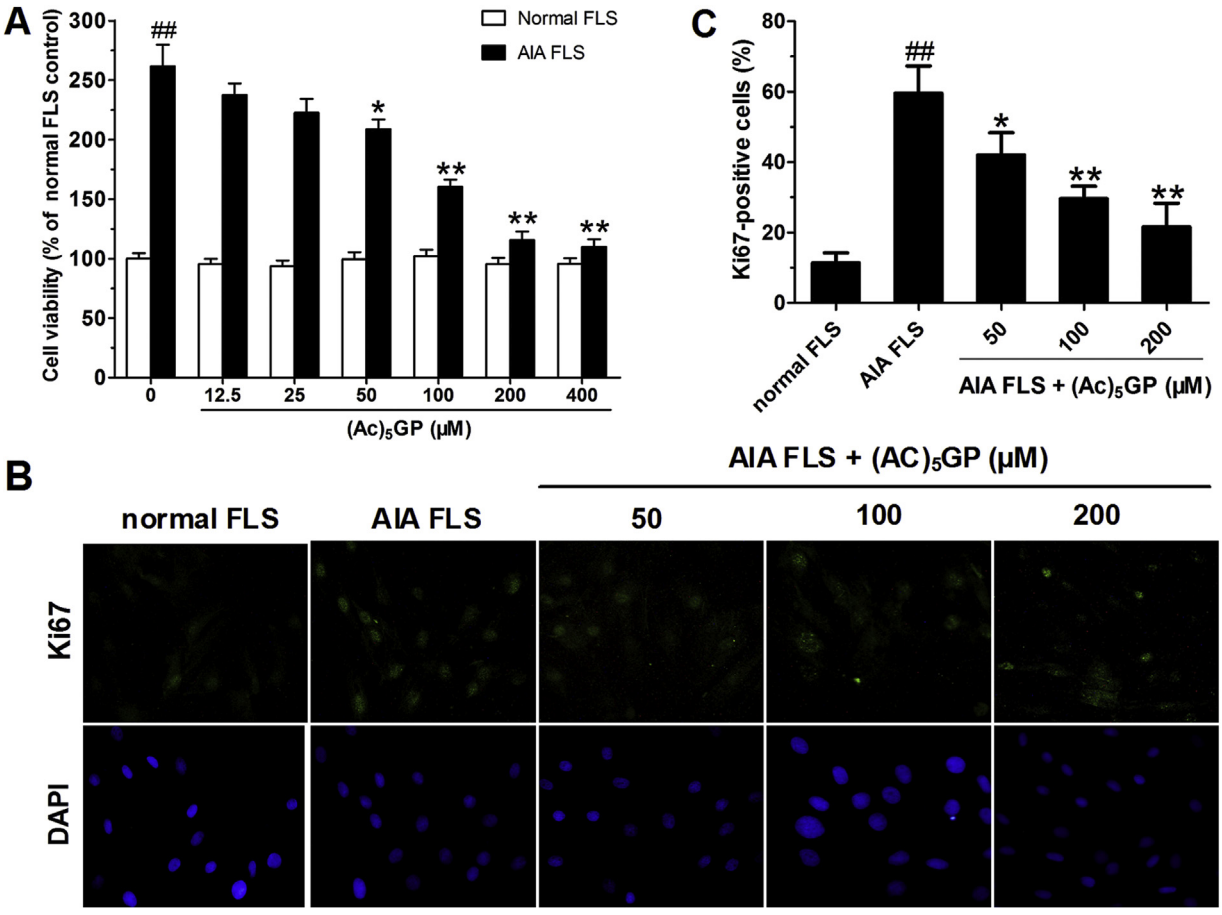


**Fig. 2.** $(Ac)_5GP$ inhibited the proliferation of AIA FLS *in vitro*. (A) Effect of $(Ac)_5GP$ on the viability of normal FLS and AIA FLS *in vitro* (MTT assay). (B) Typical photos of Ki67 immunofluorescence staining from various groups (×200). (C) Quantitative statistical results of Ki67-positive cells (%). The data are mean ± SEM of three to five independent experiments performed in triplicate. $^{\#\#}p < 0.01$ compared with normal FLS group. $^{*}p < 0.05$, $^{**}p < 0.01$ compared with AIA FLS group.

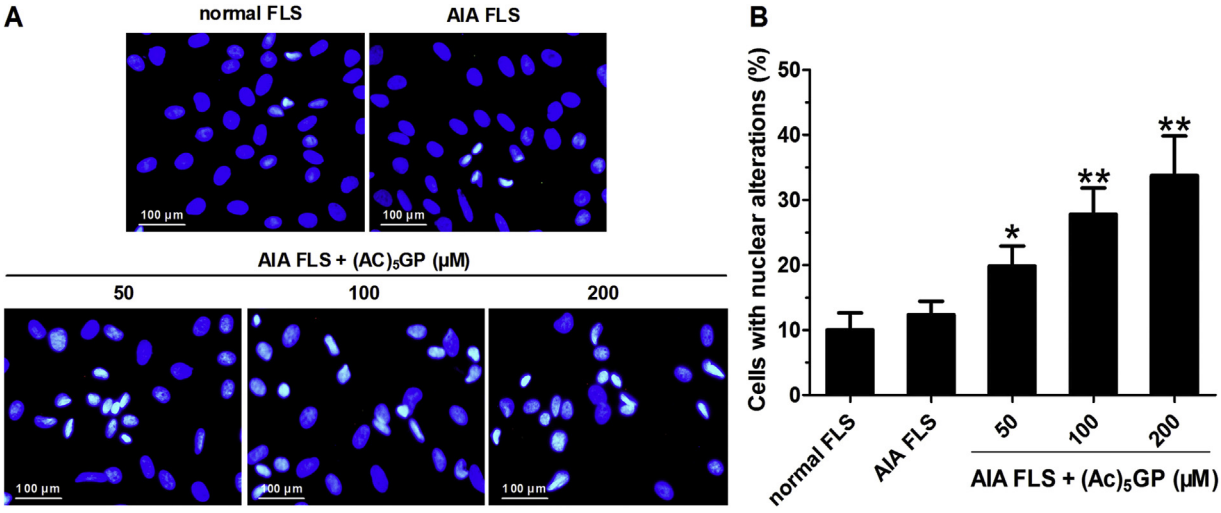


**Fig. 3.** $(Ac)_5GP$ induced apoptotic nuclear morphology in AIA FLS. (A) Typical photos of hoechst staining from various groups (×100). (B) Quantitative statistical results of the percentages of cells with nuclear alterations. The data are mean ± SEM of five independent experiments performed in triplicate. $^{*}p < 0.05$, $^{**}p < 0.01$ compared with AIA FLS group.

*$(Ac)_5GP$ regulated the protein levels of Bcl-2, Bax and caspase 3 in AIA FLS*

As shown in Fig. 6, Bcl-2 protein level in AIA FLS group was higher than that in normal FLS group, and this up-regulation of Bcl-2 expression was dose-dependently reversed by treatment of $(Ac)_5GP$ at 50,100 and 200 μM. The protein levels of Bax and caspase 3 in AIA FLS group were significantly decreased as contrasted to normal FLS group. $(Ac)_5GP$ treatment restored the reduced levels of Bax and caspase 3, with $(Ac)_5GP$ at 100 and 200 μM showing statistical significance.

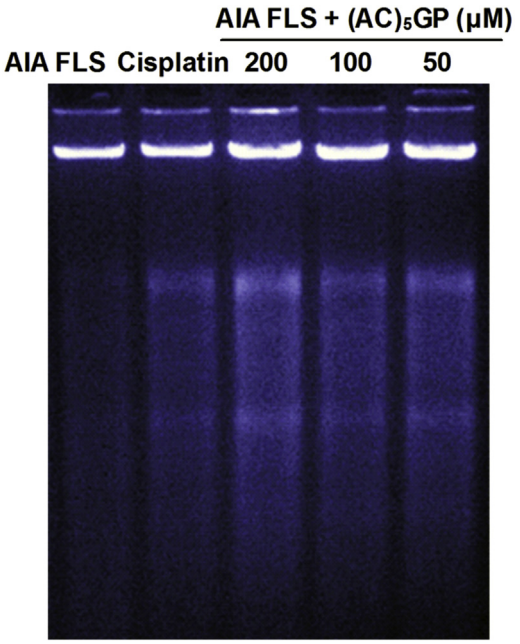


**Fig. 4.** $(Ac)_5GP$ facilitated the formation of DNA ladder pattern in AIA FLS, detected by agarose gel electrophoresis. Cisplatin was applied as a positive control.

*$(Ac)_5GP$ inhibited the activation of NF-κB signaling pathway in AIA FLS*

As shown in Fig. 7, IκBα degradation and its phosphorylation in cytoplasm of AIA FLS were significantly increased as compared with those of normal FLS. $(Ac)_5GP$ (50,100 and 200 μM) dose-dependently

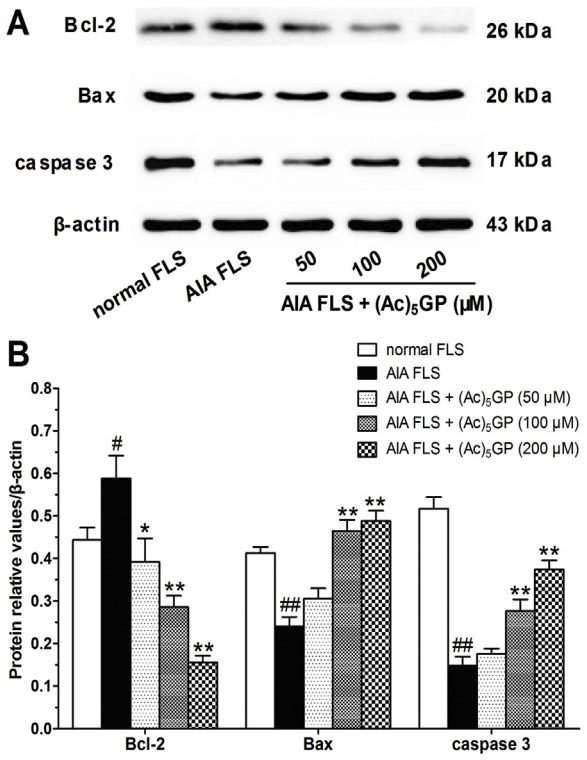


**Fig. 6.** $(Ac)_5GP$ regulated the protein levels of Bcl-2, Bax and caspase 3 in AIA FLS. (A) Typical expression examples of Bcl-2, Bax and caspase 3 from various groups (western blot assay). (B) Quantitative statistical results of the protein relative values. The data are mean ± SEM of three independent experiments performed in triplicate. $^{\#}p < 0.05$, $^{\#\#}p < 0.01$ compared with normal FLS group. $^{*}p < 0.05$, $^{**}p < 0.01$ compared with AIA FLS group.

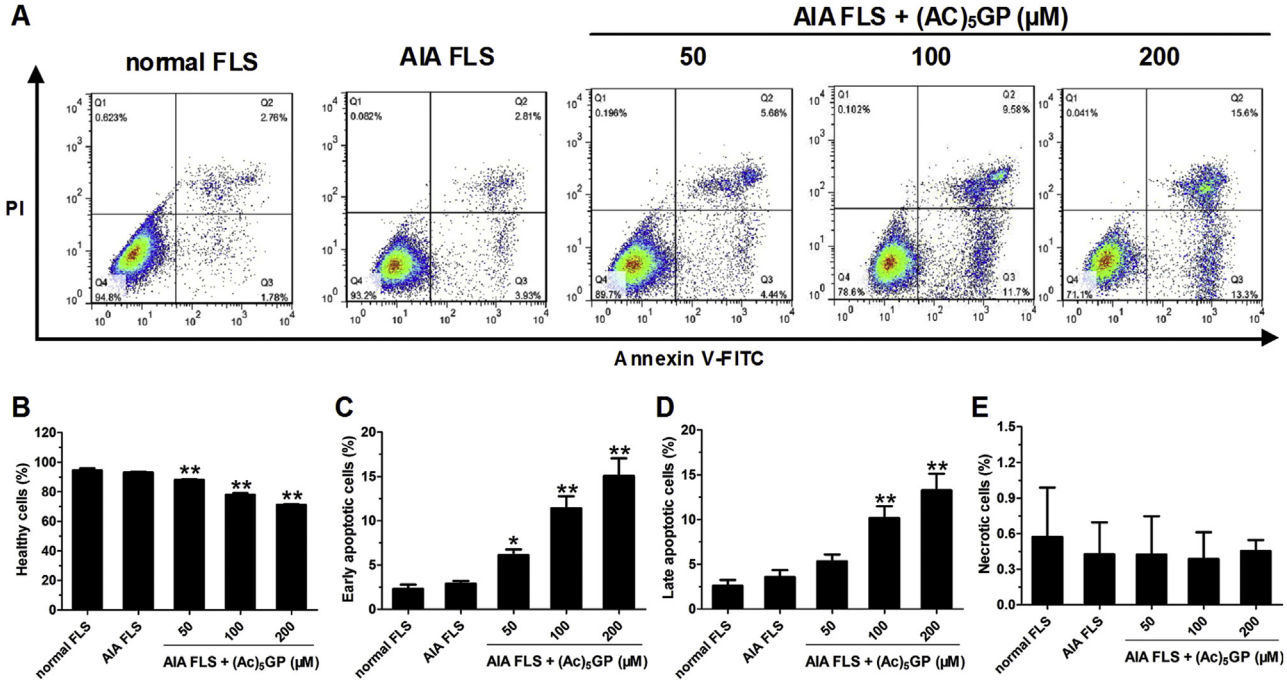


**Fig. 5.** $(Ac)_5GP$ increased AIA FLS apoptosis, detected by flow cytometer with Annexin V-FITC/PI staining. (A) Typical examples of flow cytometer results from various groups. (B–E) Quantitative statistical results of the percentages of healthy cells (B), early apoptotic cells (C), late apoptotic cells (D) and necrotic cells (E). The data are mean ± SEM of three independent experiments performed in triplicate. $^{*}p < 0.05$, $^{**}p < 0.01$ compared with AIA FLS group.

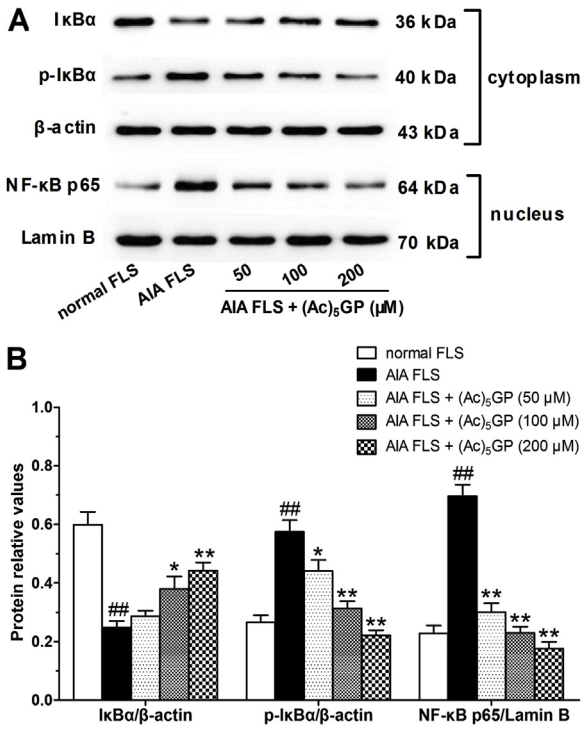


**Fig. 7.** $(Ac)_5GP$ inhibited the activation of NF-κB signaling pathway in AIA FLS. (A) Typical expression examples of IκBα, p-IκBα (in cytoplasm) and NF-κB p65 (in nucleus) from various groups (western blot assay). (b) Quantitative statistical results of the protein relative values. The data are mean ± SEM of three independent experiments performed in triplicate. $^{\#\#}p < 0.01$ compared with normal FLS group. $^{*}p < 0.05$, $^{**}p < 0.01$ compared with AIA FLS group.

suppressed the degradation as well as phosphorylation of IκBα in AIA FLS. In addition, AIA FLS had an elevated level of NF-κB p65 protein in nucleus than normal FLS. $(Ac)_5GP$ treatment on AIA FLS significantly reversed this raised level of NF-κB p65 protein in nucleus.

### *$(Ac)_5GP$ suppressed NF-κB p65 nuclear translocation in AIA FLS*

In Fig. 8, NF-κB p65 in normal FLS was principally located in cytoplasm and rarely expressed in nucleus. Contrarily, enhanced NF-κB p65 staining in nucleus was observed in AIA FLS, suggesting augmented NF-κB p65 nuclear translocation in AIA FLS. $(Ac)_5GP$ (50,100 and 200 μM) treatment on AIA FLS suppressed the nuclear translocation of NF-κB p65 at varying degrees.

## Discussion

CFA-induced rat AIA is a classic experimental model resembling RA. This model is widely used to explore RA pathogenesis and screen potential therapeutic drugs [15]. The application of natural products in RA treatment has attracted increasing attention. We recently revealed that $(Ac)_5GP$ (an active derivative of geniposide) exhibited an anti-arthritic effect on AIA rats *in vivo* by reducing the levels of pro-inflammatory cytokines and inhibiting the hyperplasia of synovial tissues [10]. Interestingly, the anti-proliferative and pro-apoptotic effects of $(Ac)_5GP$ on cancer cells has been reported in tumor studies [12,13]. Here, the cells cultured from rat synovial tissues were identified as FLS by the long spindle cell morphology and the positive VCAM-1 staining. The present study aimed to demonstrate the pro-apoptotic potential of $(Ac)_5GP$ on AIA FLS *in vitro* and explore the involved molecular mechanisms.

It has been found that geniposide (the parent compound of $(Ac)_5GP$) at 64.4, 128.8 and 257.6 μM showed anti-inflammatory effect on LPS-stimulated mouse mammary epithelial cells [16]. Another *in vitro* work reported that geniposide at 128.8, 257.6 and 515.2 μM dose-dependently decreased the levels of TNF-α, IL-6 and IL-1β in LPS-stimulated mouse macrophages [17]. $(Ac)_5GP$ at the concentrations of ranged from 150 to 600 μM was used in a series of previous studies on its pro-apoptotic effect on C6 glioma cells [11–13]. In this study, we evaluated the effect of $(Ac)_5GP$ on normal FLS and AIA FLS at various concentrations of 0, 12.5, 25, 50, 100, 200 and 400 μM by MTT assay. $(Ac)_5GP$ at above concentrations for 48 h showed no obvious effect on normal FLS viability. However, $(Ac)_5GP$ significantly reduced AIA FLS viability at

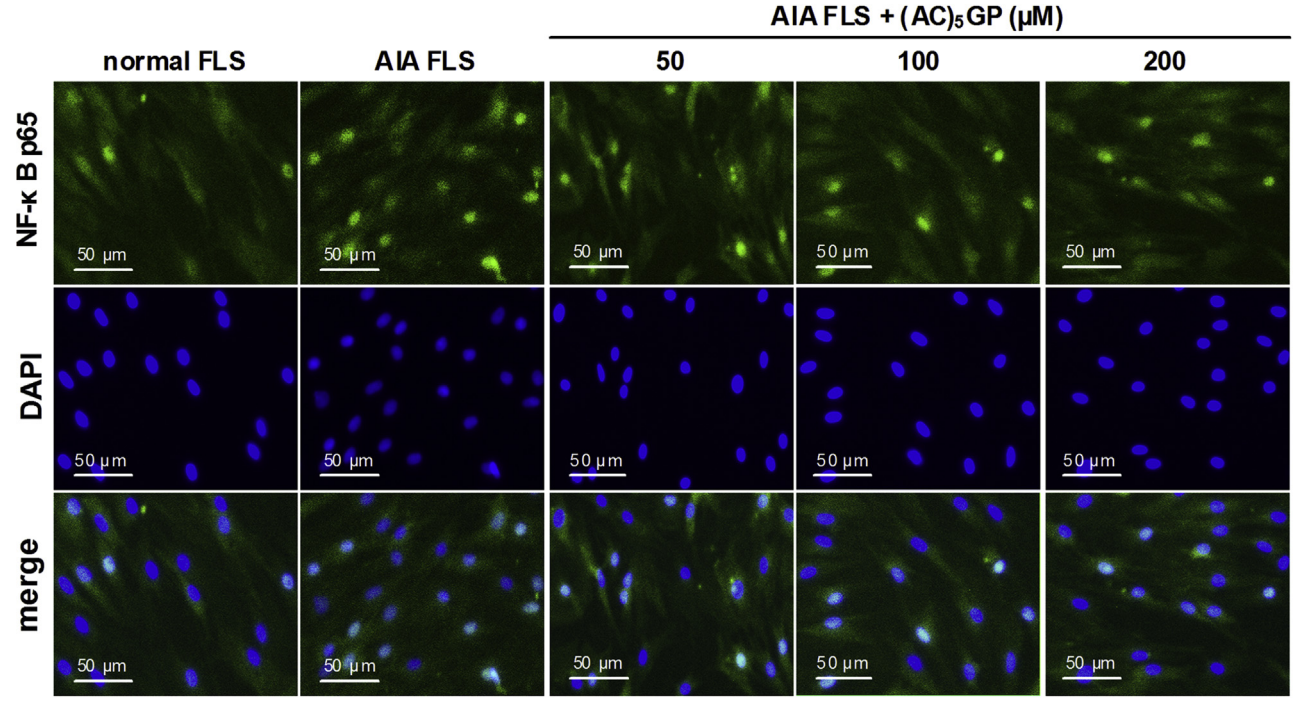


**Fig. 8.** $(Ac)_5GP$ suppressed NF-κB p65 nuclear translocation in AIA FLS, detected by immunofluorescence staining assay (×200).

concentrations of 50, 100, 200 and 400 μM as compared with AIA FLS control group. Since the inhibitory effect had no significant difference between $(Ac)_5GP$ 200 μM and $(Ac)_5GP$ 400 μM, the concentrations of $(Ac)_5GP$ (50, 100 and 200 μM) were adopted for the following experiments in AIA FLS.

The insufficient or disorderly apoptosis of RA FLS contribute to the continuous thickness of synovial membrane lining and is a crucial pathological change in RA development. Interventions aimed to promote FLS apoptosis may be a meaningful strategy for RA treatment [18]. Herein, a series of assays was combinedly used to detect the anti-proliferative and pro-apoptotic effects of $(Ac)_5GP$ on AIA FLS *in vitro*. MTT assay results revealed that $(Ac)_5GP$ treatment reduced the viability of AIA FLS, with no effect on the viability of normal FLS. Ki67 expressed in all cell cycle phases except G0 is a commonly used cellular marker of proliferation [19], and $(Ac)_5GP$ treatment decreased the percentage of Ki67-positive cells in AIA FLS. The nuclear morphology changes including nuclear fragmentation and chromatin condensation are the typical characteristics of apoptotic cells [20]. Hoechst staining indicated that $(Ac)_5GP$ treatment on AIA FLS increased the percentage of apoptotic cells with nuclear alterations. DNA fragmentation is well known as the hallmark of cell apoptosis [21], and the formation of DNA ladder could be easily found in AIA FLS treated with $(Ac)_5GP$. Annexin V-FITC/PI staining further revealed that $(Ac)_5GP$ apparently increased the percentages of both early and late apoptotic cells in AIA FLS. The above data clearly showed that $(Ac)_5GP$ could effectively inhibit the proliferation and promote the apoptosis of AIA FLS *in vitro*, which may be closely involved in its anti-arthritic effect on rat AIA *in vivo* [10].

Bcl-2 family proteins are the vital regulators in the mitochondria-initiated caspase activation pathway [22]. Bcl-2 can reduce cell apoptosis by inhibiting the release of apoptosis-inducing factors from mitochondria to cytoplasm and keeping the integrity of mitochondrial membrane [23]. On the contrary, Bax promotes cell apoptosis by stimulating cytochrome C release and inducing mitochondrial depolarization [24]. The mitochondria damage causes the activation of caspase family. As a key member of caspase family, caspase 3 acts as the most important apoptosis executor by cleaving critical cellular proteins [25]. In this study, elevated expression of Bcl-2 protein and reduced expression of Bax and caspase 3 proteins were found in AIA FLS. $(Ac)_5GP$ treatment decreased the level of Bcl-2 and increased the levels of Bax and caspase 3. The regulatory effect of $(Ac)_5GP$ on the expression of these apoptosis-related proteins is intimately linked with $(Ac)_5GP$-induced apoptosis of AIA FLS.

NF-κB signaling modulates the expression of cytokines, enzymes and adhesion molecules, all of which affect various cellular responses including inflammation, immunity, proliferation and apoptosis [26]. Over-activated NF-κB is involved in the inflammatory response in RA, and contributes to the excessive synovial hyperplasia by increasing proliferation and inhibiting apoptosis of FLS [27]. Inhibition of NF-κB takes effect in suppressing inflammation response and synovial hyperplasia in RA, and can be regarded as an effective approach for RA therapy [28]. Similar to previous findings [29], NF-κB was over-activated in AIA FLS contrasted to normal FLS in the present study. $(Ac)_5GP$ treatment could effectively suppress the activation of NF-κB in AIA FLS, indicating that the pro-apoptotic effect of $(Ac)_5GP$ may be associated with inhibition of NF-κB signaling pathway. In addition, AIA FLS produced higher levels of TNF-α and IL-1β than normal FLS, while $(Ac)_5GP$ (200 μM) treatment remarkably reduced the levels of TNF-α and IL-1β as contrasted to AIA FLS group (data shown in the Supplement), suggesting an anti-inflammatory effect of $(Ac)_5GP$ on AIA FLS *in vitro*. This inhibitory effect of $(Ac)_5GP$ on TNF-α and IL-1β *in vitro* is consistent with the finding in our *in vivo* study [10]. As we known, NF-κB activation can induce the expression of multiple pro-inflammatory mediators including COX2, iNOS, TNF-α and IL-1β. The increased pro-inflammatory cytokines in turn potently activate the NF-κB signaling pathway, thus forming a positive circle of each other [30]. In this study, the inhibition of $(Ac)_5GP$ on NF-κB activation *in vitro* might be partly attributed to its inhibitory effect on the productions of TNF-α and IL-1β. It should be mentioned that besides NF-κB other signaling pathways (e.g., PI3K/Akt and MAPK) may also contribute to the pro-apoptotic effect of $(Ac)_5GP$. Activated MAPK has been found to be related to $(Ac)_5GP$-induced apoptosis in C6 glioma cells, by mediating AP-1 activation and the downstream apoptotic signals [13]. Moreover, $(Ac)_5GP$ exerted anti-proliferative and anti-metastastic effect on C6 glioma cells by inhibiting PI3K protein expression, ERK phosphorylation and activation of transcription factors (NF-κB, c-Fos, c-Jun) [11]. Further detailed works are needed to fully clarify the molecular events implicated in the pro-apoptotic actions of $(Ac)_5GP$ on AIA FLS both *in vitro* and *in vivo*.

In conclusion, $(Ac)_5GP$ inhibited the proliferation of AIA FLS effectively by promoting cell apoptosis *in vitro*. $(Ac)_5GP$ exerted its pro-apoptotic effect related to regulating the expression of apoptosis-related proteins and suppressing the activation of NF-κB signaling pathway. It is reasonable to take $(Ac)_5GP$ as a potential alternative agent for RA treatment.

## Conflict of interest

The authors declare no conflict of interest.

## Acknowledgment

This work was supported by National Natural Science Foundation of China (81102273, 81201052), Program for Outstanding Young Talents of Higher Education Institution of Anhui Province (gxyqZD2016045) and Program for the Young and Middle-aged Academic Technology Leaders of Anhui Medical University (201309).

## References

[1] McInnes IB, Schett G. The pathogenesis of rheumatoid arthritis. N Engl J Med 2011;365:2205–19.
[2] Bartok B, Firestein GS. Fibroblast-like synoviocytes: key effector cells in rheumatoid arthritis. Immunol Rev 2010;233:233–55.
[3] Smith MD, Weedon H, Papangelis V, Walker J, Roberts-Thomson PJ, Ahern MJ. Apoptosis in the rheumatoid arthritis synovial membrane: modulation by disease-modifying anti-rheumatic drug treatment. Rheumatology (Oxford) 2010;49:862–75.
[4] Pope RM. Apoptosis as a therapeutic tool in rheumatoid arthritis. Nat Rev Immunol 2002;2:527–35.
[5] Ding H, Gao G, Zhang L, Shen G, Sun W, Gu Z, et al. The protective effects of curculigoside A on adjuvant-induced arthritis by inhibiting NF-small ka, CyrillicB/NLRP3 activation in rats. Int Immunopharmacol 2016;30:43–9.
[6] Shan M, Yu S, Yan H, Guo S, Xiao W, Wang Z, et al. A review on the phytochemistry, pharmacology, pharmacokinetics and toxicology of geniposide, a natural product. Molecules 2017;22.
[7] Chen JY, Wu H, Li H, Hu SL, Dai MM, Chen J. Anti-inflammatory effects and pharmacokinetics study of geniposide on rats with adjuvant arthritis. Int Immunopharmacol 2015;24:102–9.
[8] Wang F, Cao J, Hao J, Liu K. Pharmacokinetics, bioavailability and tissue distribution of geniposide following intravenous and peroral administration to rats. Biopharm Drug Dispos 2014;35:97–103.
[9] Zhang H, Shi T, Wang J, Li R, Tang W. Protective effect of penta-acetyl geniposide on acute liver injury induced by D-galactosamine in mice. Br J Pharmacol Toxicol. 2013;4:256–61.
[10] Cai L, Li CM, Tang WJ, Liu MM, Chen WN, Qiu YY, et al. Therapeutic effect of penta-acetyl geniposide on adjuvant-induced arthritis in rats: involvement of inducing synovial apoptosis and inhibiting NF-kappaB signal pathway. Inflammation 2018;41:2184–95.
[11] Huang HP, Shih YW, Wu CH, Lai PJ, Hung CN, Wang CJ. Inhibitory effect of penta-acetyl geniposide on C6 glioma cells metastasis by inhibiting matrix metalloproteinase-2 expression involved in both the PI3K and ERK signaling pathways. Chem Biol Interact 2009;181:8–14.
[12] Peng CH, Huang CN, Hsu SP, Wang CJ. Penta-acetyl geniposide induce apoptosis in C6 glioma cells by modulating the activation of neutral

sphingomyelinase-induced p75 nerve growth factor receptor and protein kinase Cdelta pathway. Mol Pharmacol 2006;70:997–1004.
[13] Peng CH, Huang CN, Hsu SP, Wang CJ. Penta-acetyl geniposide-induced apoptosis involving transcription of NGF/p75 via MAPK-mediated AP-1 activation in C6 glioma cells. Toxicology 2007;238:130–9.
[14] Narendhirakannan RT, Limmy TP. Anti-inflammatory and anti-oxidant properties of Sida rhombifolia stems and roots in adjuvant induced arthritic rats. Immunopharmacol Immunotoxicol 2012;34:326–36.
[15] Bilasy SE, Essawy SS, Mandour MF, Ali EA, Zaitone SA. Myelosuppressive and hepatotoxic potential of leflunomide and methotrexate combination in a rat model of rheumatoid arthritis. Pharmacol Rep 2015;67:102–14.
[16] Song X, Zhang W, Wang T, Jiang H, Zhang Z, Fu Y, et al. Geniposide plays an anti-inflammatory role via regulating TLR4 and downstream signaling pathways in lipopolysaccharide-induced mastitis in mice. Inflammation 2014;37:1588–98.
[17] Fu Y, Liu B, Liu J, Liu Z, Liang D, Li F, et al. Geniposide, from Gardenia jasminoides Ellis, inhibits the inflammatory response in the primary mouse macrophages and mouse models. Int Immunopharmacol 2012;14:792–8.
[18] Zou S, Wang C, Cui Z, Guo P, Meng Q, Shi X, et al. Beta-Elemene induces apoptosis of human rheumatoid arthritis fibroblast-like synoviocytes via reactive oxygen species-dependent activation of p38 mitogen-activated protein kinase. Pharmacol Rep 2016;68:7–11.
[19] Kukolj T, Trivanovic D, Mojsilovic S, Okic Djordjevic I, Obradovic H, Krstic J, et al. IL-33 guides osteogenesis and increases proliferation and pluripotency marker expression in dental stem cells. Cell Prolif 2019;52:e12533.
[20] Ishimura A, Ng JK, Taira M, Young SG, Osada S. Man1, an inner nuclear membrane protein, regulates vascular remodeling by modulating transforming growth factor beta signaling. Development 2006;133:3919–28.
[21] Ahamad MS, Siddiqui S, Jafri A, Ahmad S, Afzal M, Arshad M. Induction of apoptosis and antiproliferative activity of naringenin in human epidermoid carcinoma cell through ROS generation and cell cycle arrest. PLoS One 2014;9:e110003.
[22] Eichhorn JM, Alford SE, Sakurikar N, Chambers TC. Molecular analysis of functional redundancy among anti-apoptotic Bcl-2 proteins and its role in cancer cell survival. Exp Cell Res 2014;322:415–24.
[23] Leber B, Lin J, Andrews DW. Embedded together: the life and death consequences of interaction of the Bcl-2 family with membranes. Apoptosis 2007;12:897–911.
[24] Crompton M. Bax, Bid and the permeabilization of the mitochondrial outer membrane in apoptosis. Curr Opin Cell Biol 2000;12:414–9.
[25] Sabine VS, Faratian D, Kirkegaard-Clausen T, Bartlett JM. Validation of activated caspase-3 antibody staining as a marker of apoptosis in breast cancer. Histopathology 2012;60:369–71.
[26] Tak PP, Firestein GS. NF-kappaB: a key role in inflammatory diseases. J Clin Invest 2001;107:7–11.
[27] Simmonds RE, Foxwell BM. Signalling, inflammation and arthritis: NF-kappaB and its relevance to arthritis and inflammation. Rheumatology (Oxford) 2008;47:584–90.
[28] van Loo G, Beyaert R. Negative regulation of NF-kappaB and its involvement in rheumatoid arthritis. Arthritis Res Ther 2011;13:221.
[29] Chen Y, Xian PF, Yang L, Wang SX. MicroRNA-21 promotes proliferation of fibroblast-Like synoviocytes through mediation of NF-kappaB nuclear translocation in a rat model of collagen-induced rheumatoid arthritis. Biomed Res Int 2016;2016:9279078.
[30] Park MH, Hong JT. Roles of NF-kappaB in cancer and inflammatory diseases and their therapeutic approaches. Cells 2016;5.